



NANTEN
Submillimeter Observatory

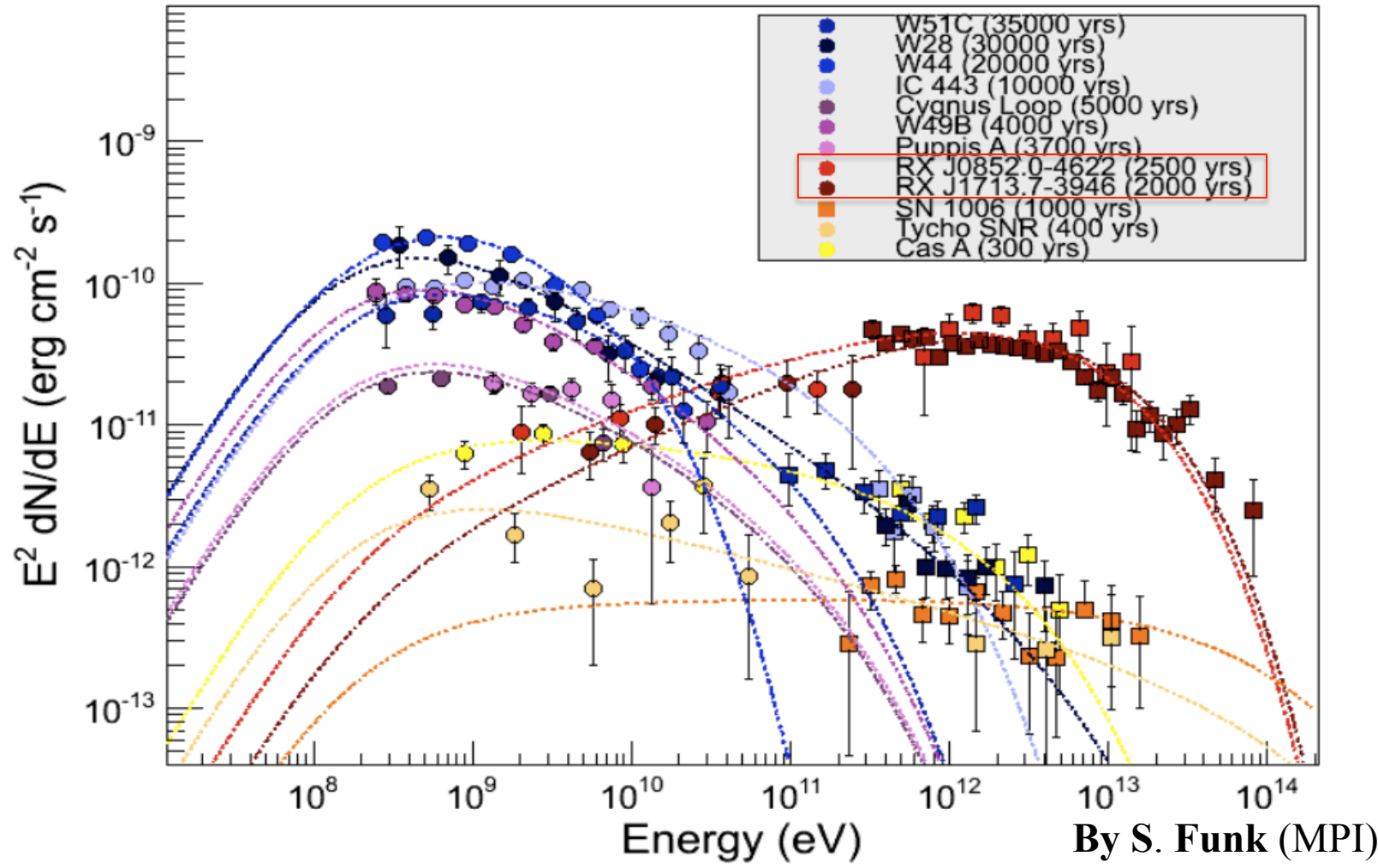
特別推進研究研究会・宇宙線研究所共同利用研究会
「高エネルギーガンマ線でみる極限宇宙2013」
2013年9月4日(火) 東京大学 柏キャンパス

NANTEN2 と Suzaku 衛星による 若いTeVガンマ線SNRの研究

佐野 栄俊 (Hidetoshi SANO; 名大理 D3)

共同研究者：福田達哉, 吉池智史, 鳥居和史, 早川貴敬, 山本宏昭, 立原研悟, 犬塚修一郎, 福井康雄 (名大理), 田中孝明 (京大理), 松本浩典 (名大KMI), 内山泰伸 (立教大理), 井上剛志, 山崎了 (青山学院大理), 河村晶子, 水野範和 (NAOJ), 水野亮 (名大STE), 西村淳, 大西利和 (大阪府立大理), 他NANTENチーム

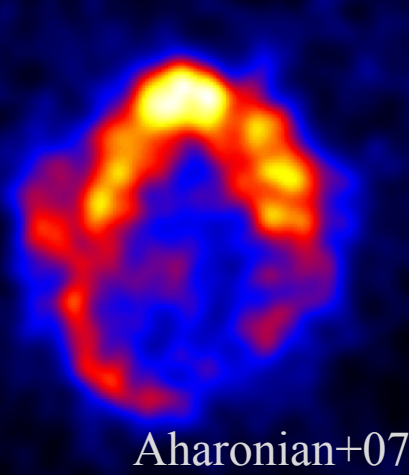
- SNRにおける Cosmic-Rays (CRs) の加速は、ほぼ揺るぎないものに (e.g., Fermi results)
→しかし、本当に Knee energy 付近まで CRs は加速されているのか？



- 若く (~2000yr) TeV ガンマ線で明るい SNR が、現段階ではこの鍵を握る最有力ターゲット

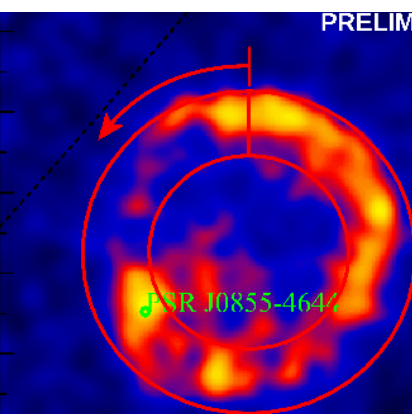
- 年齢2000年程度の4つのTeVガンマ線SNRs
→ どの天体もISM (Interstellar Medium) との相互作用が確認

RX J1713.7–3946



Aharonian+07

RX J0852.0–4622

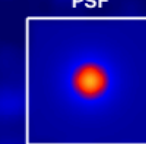


Arribas+11

PRELIMINAR

H.E.S.S.

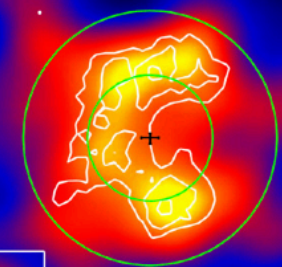
HESS J1731–347



PSF

Abramowski+11

RCW 86



Aharonian+09

視直径: ~1 deg.

年齢: ~1600 yr

ISM: rich CO + cold HI

X-rays: pure synchrotron

~2 deg.

~1700–4300 yr

rich HI + little CO

pure synchrotron ?

~0.5 deg.

~3600–7200 yr

rich CO + HI cavity

pure synchrotron

~0.5 deg.

~1800 yr

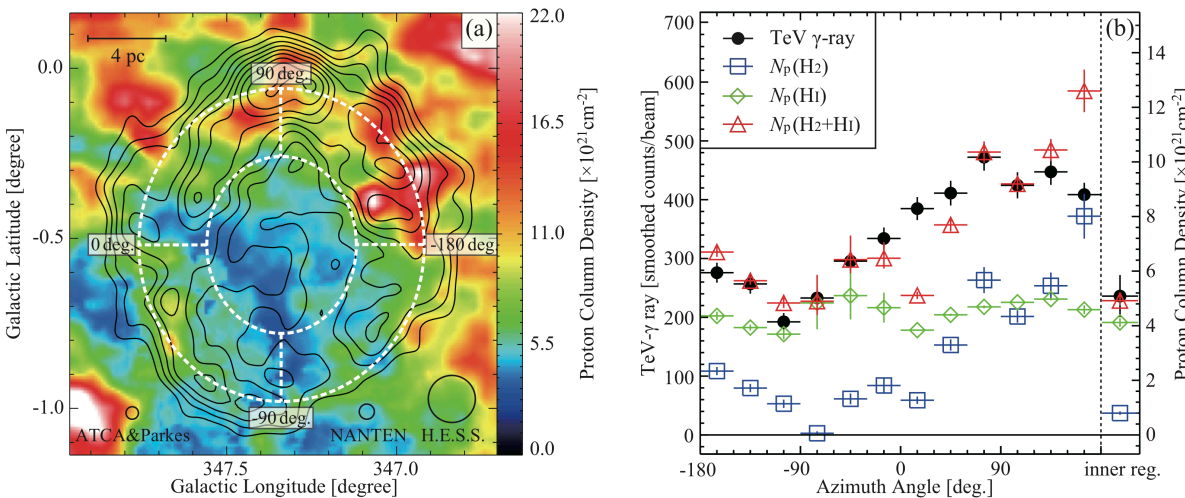
rich HI + little CO

thermal + non-thermal

- これらの高エネルギー放射起源や効率の良いCRs 加速と, ISMが密接に関係

Four TeV Gamma-ray SNRs

- RXJ1713, Vela Jr. HESSJ1731 のTeV γ 線とISMの相関



$$F \propto \frac{W_p n}{d^2}$$

W_p Total energy in accelerated protons
 n Target ISM proton density
 d Distance to the SNR

↑ e.g., RXJ1713 (Fukui, Sano et al. 2012) 高度に非一様なISM分布
 CRs proton の加速効率は ~0.1 % ($\sim 10^{48} \text{ erg}$)

- しかしながら、この空間分解能で議論できるのは視直径の大きなSNRに限られる。
 → CTA時代まで待つか、いま我々が他にできることは？

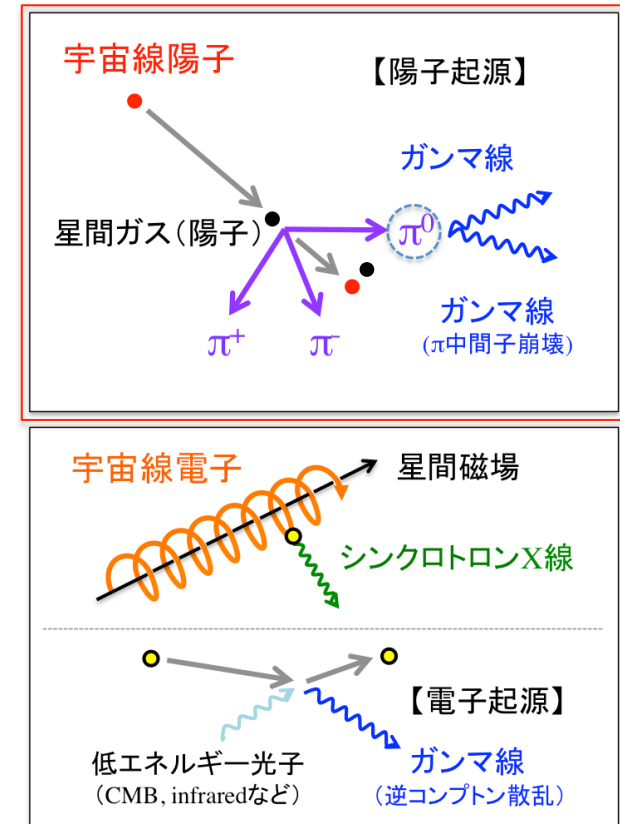
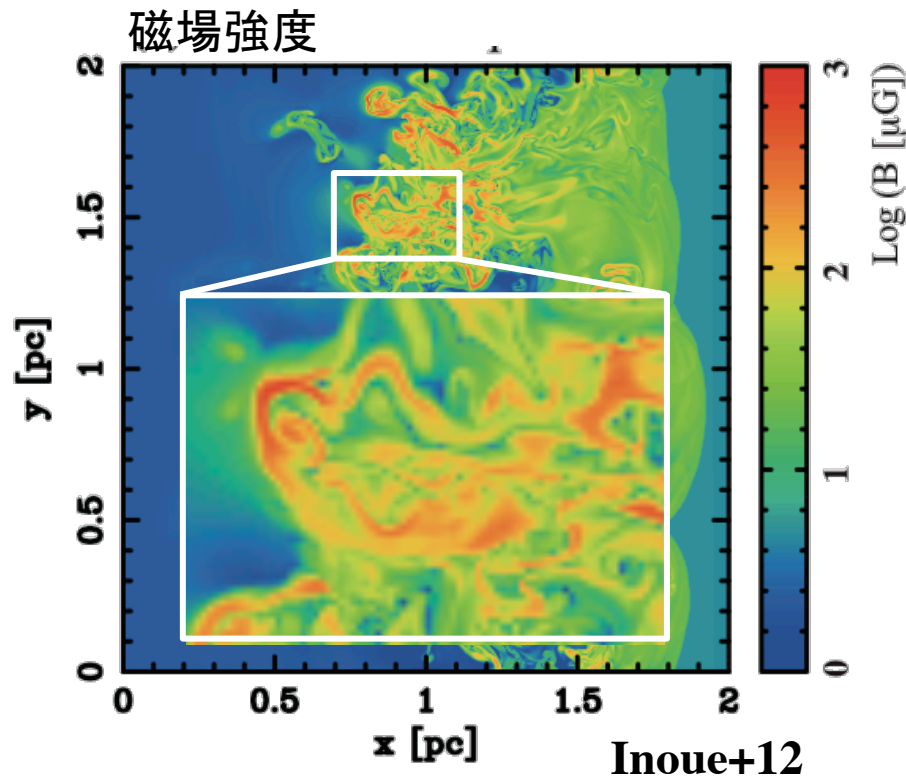
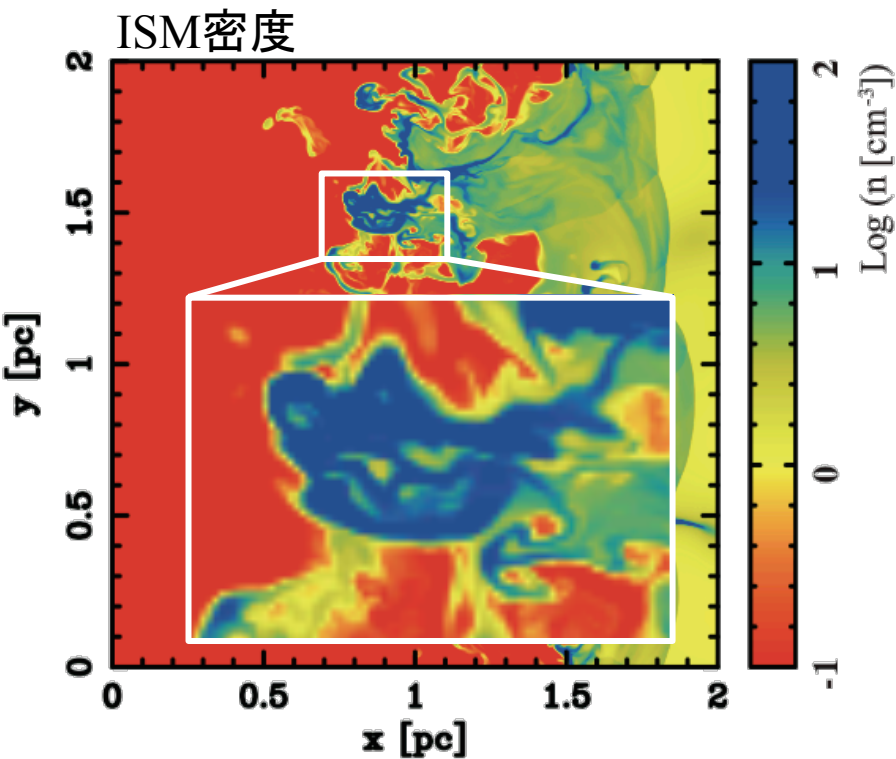


図1: 宇宙線起源の高エネルギー放射模式図

- SNR shock waves と ISM の相互作用 (Shock-cloud interaction)
⇒ ISM clump 周辺で乱流励起 + 磁場増幅
⇒ 観測的には clump 周辺のX線増光として確認できる

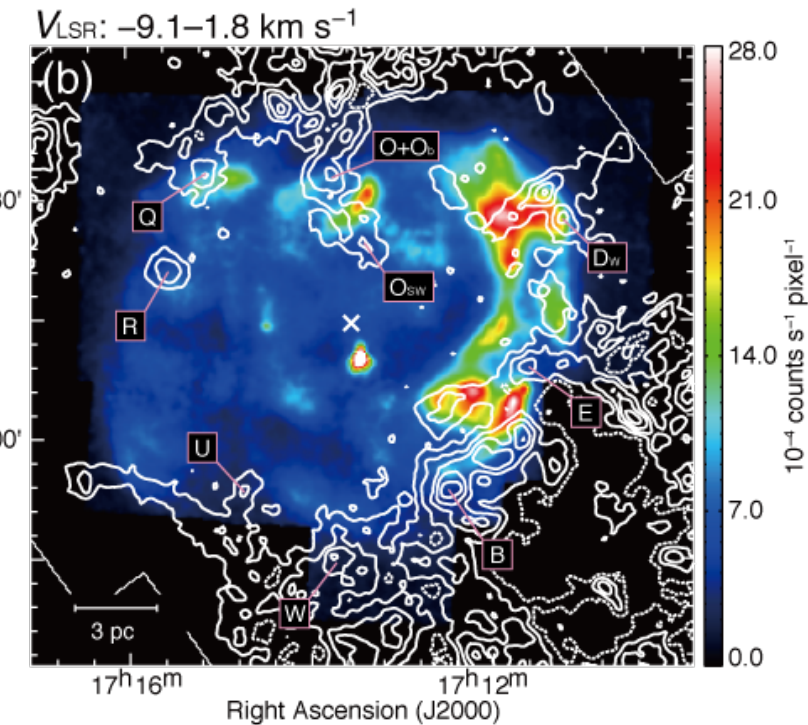
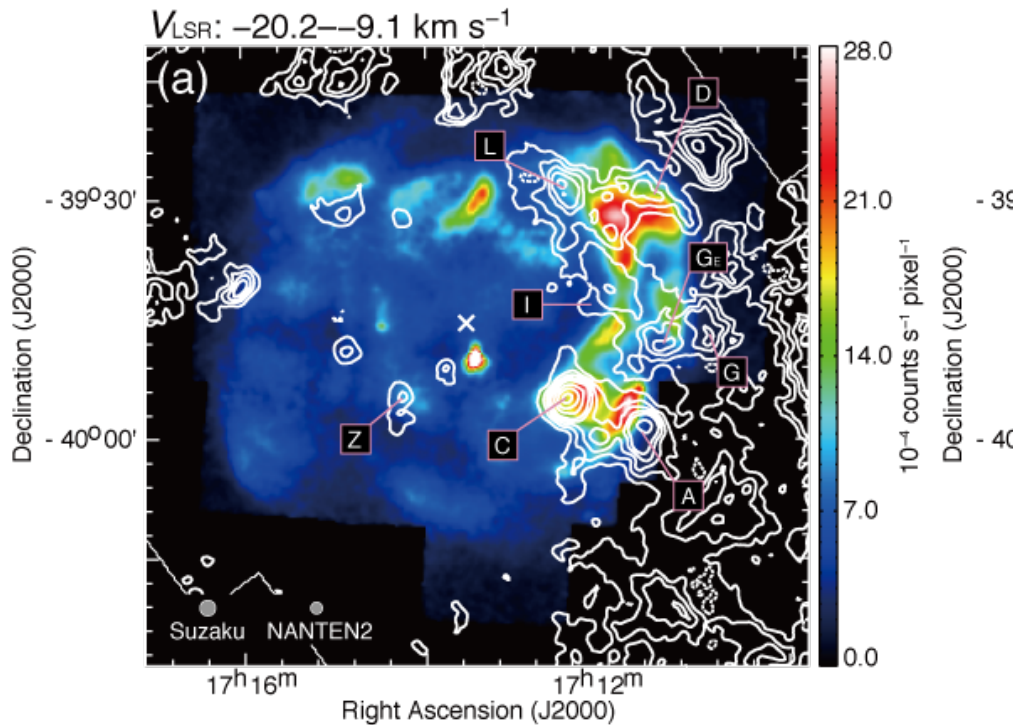


高空間分解能 / 高統計のX線データ + SNR と相互作用する ISM
CR electron acceleration についての知見を深める

- TeV ガンマ線 SNRの中でも最も重要なターゲットの1つ
⇒ Rich CO + Cold HIとの相互作用, Pure Synchrotron X-rays, 視直径 ~1 deg.

NANTEN2 CO HPBW ~1.5–3 arcmin
 Suzaku X-rays HPD ~2 arcmin
 ATCA & Parkes HI HPBW ~2.2 arcmin

Sano+13a arXiv: 1304.7722

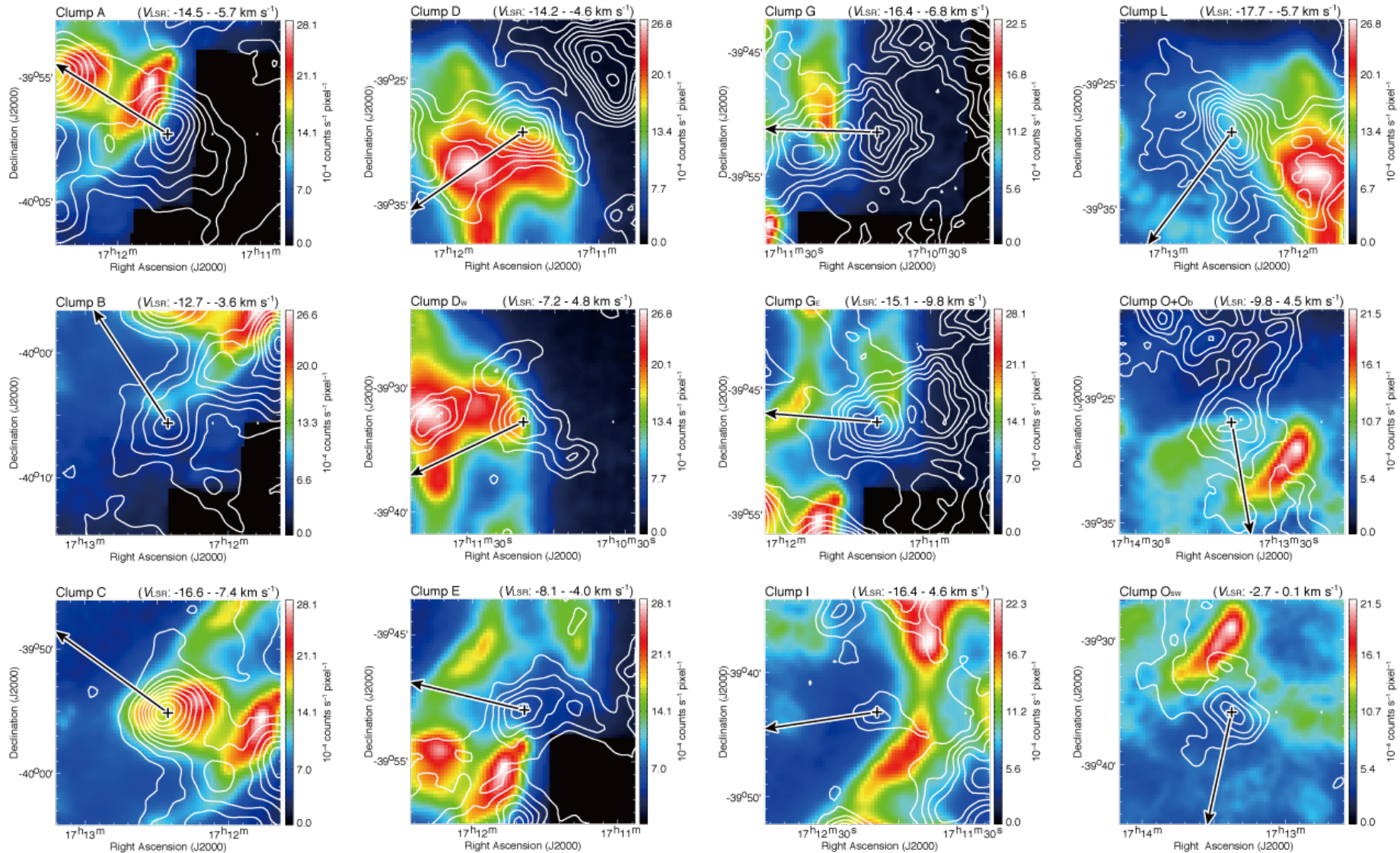


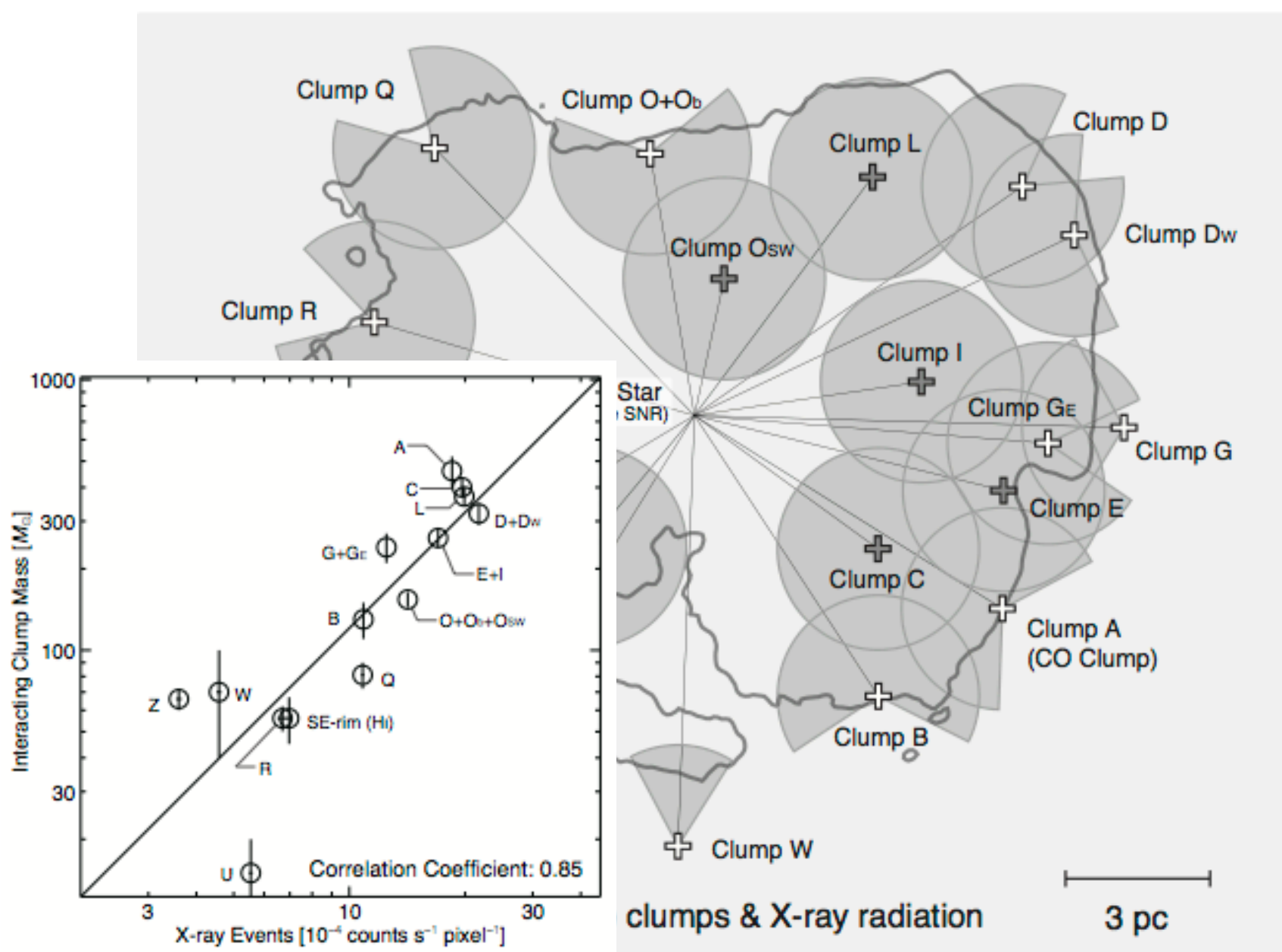
images: *Suzaku* 1–5 keV mosaics, contours: $^{12}\text{CO}(J=2-1)$ integrated intensity (two velocity ranges)

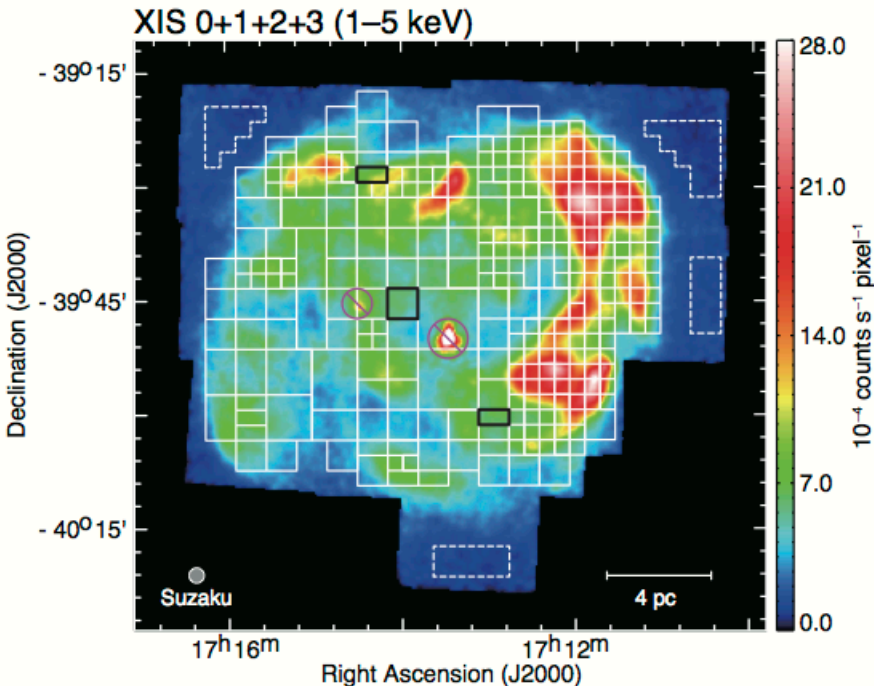
RXJ1713: Morphology (sub pc scale anti-correlation)

7/21

- 17 clumps 全てで, CO と X-ray の anti-correlation がみえている





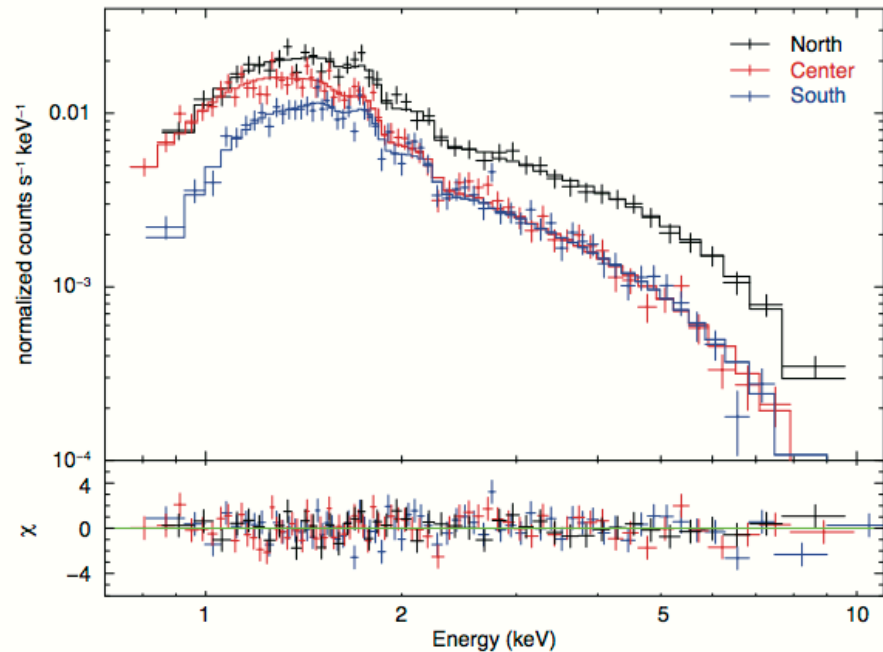


↑ Image: *Suzaku* XIS (1—5 keV) mosaic

Solid boxes: source regions

Dashed boxes: background regions

Typical X-ray spectra ↗
and best fit parameters →



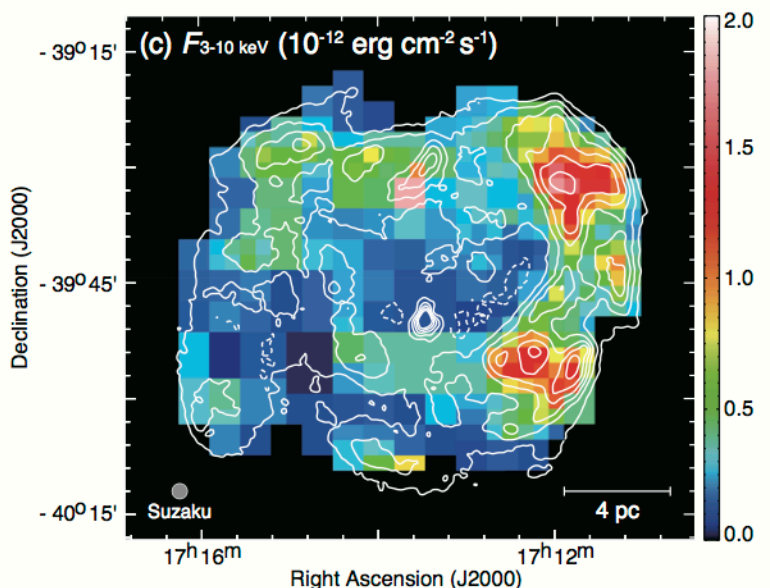
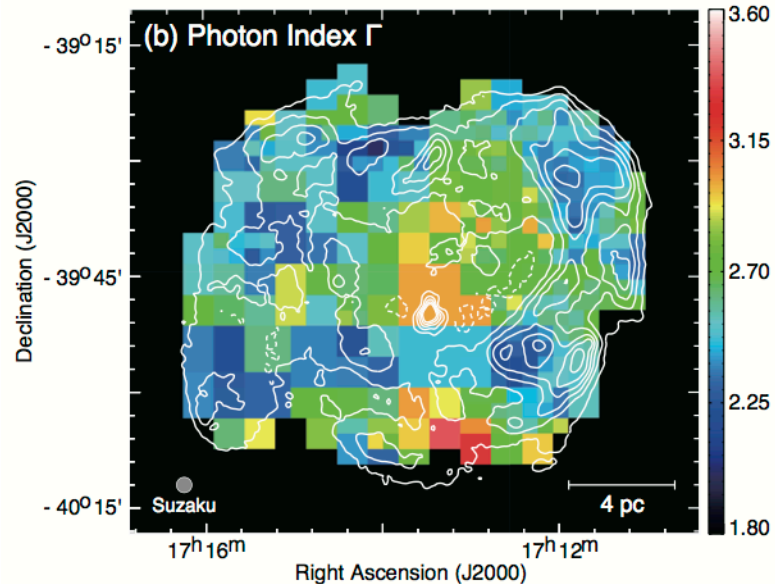
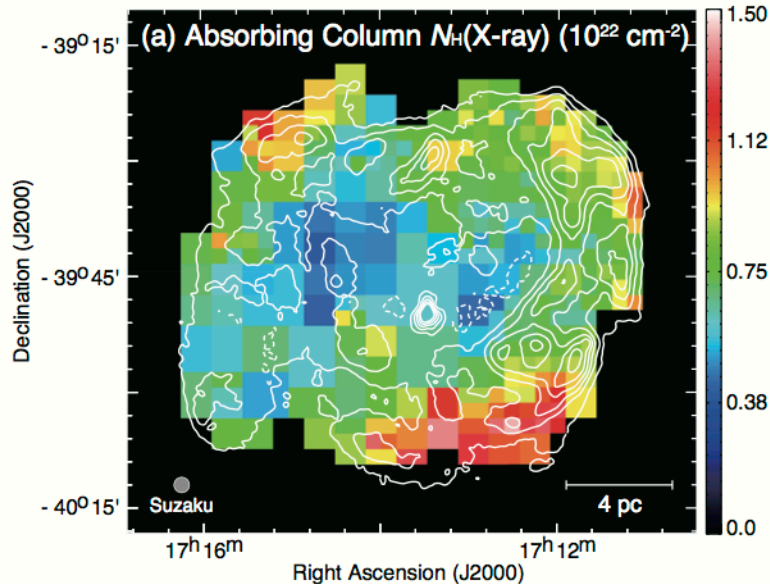
Region	N_{H} (X-ray)	Γ
North	$0.6^{+0.1}_{-0.2} \times 10^{22} \text{ cm}^{-2}$	2.1 ± 0.1
Center	$0.50^{+0.06}_{-0.05} \times 10^{22} \text{ cm}^{-2}$	2.7 ± 0.1
South	$0.89 \pm 0.09 \times 10^{22} \text{ cm}^{-2}$	2.7 ± 0.1

- Source grid size 2'–8', 計315領域からスペクトルを抽出 (FI CCDs only).
→ Absorbing column density N_{H} (X-ray) の relativistic error < 30 % となるように調整.
- Absorbed power-low model で fitting (at least ~ 100 counts / bin).

Sano+13b in prep.

X-ray Spectroscopy: Spatial and spectral characterization

10/21

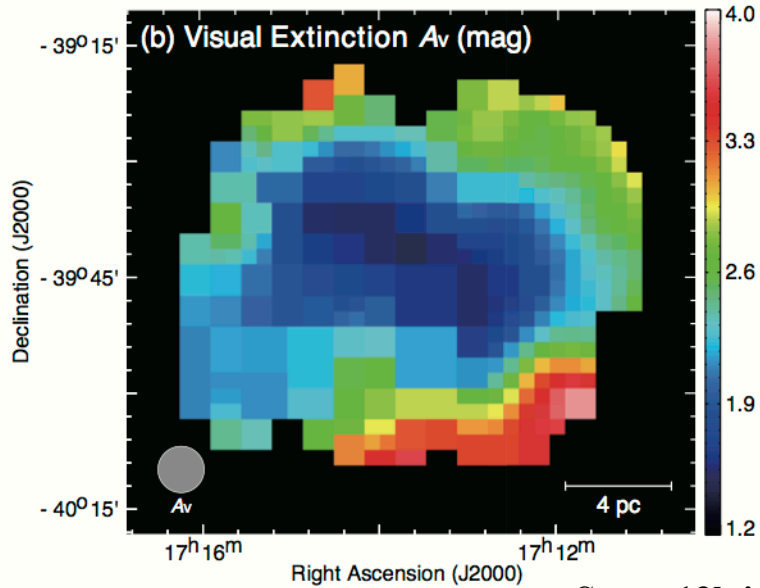
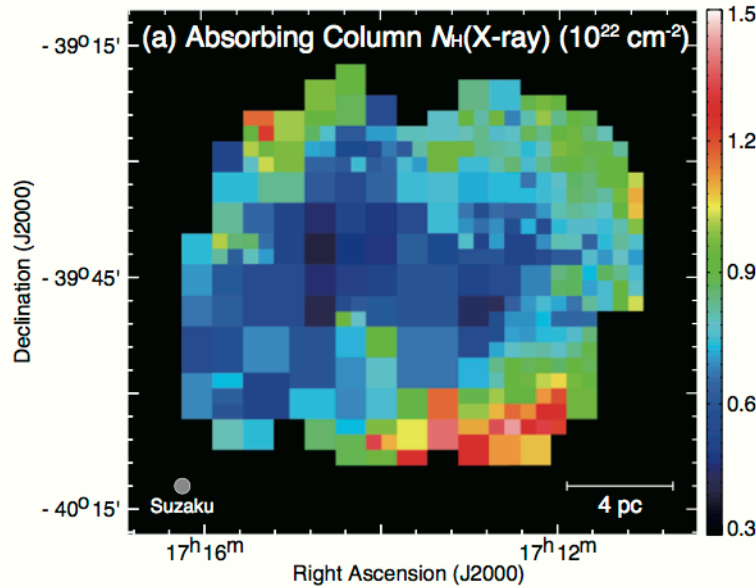


Sano+13b in prep.

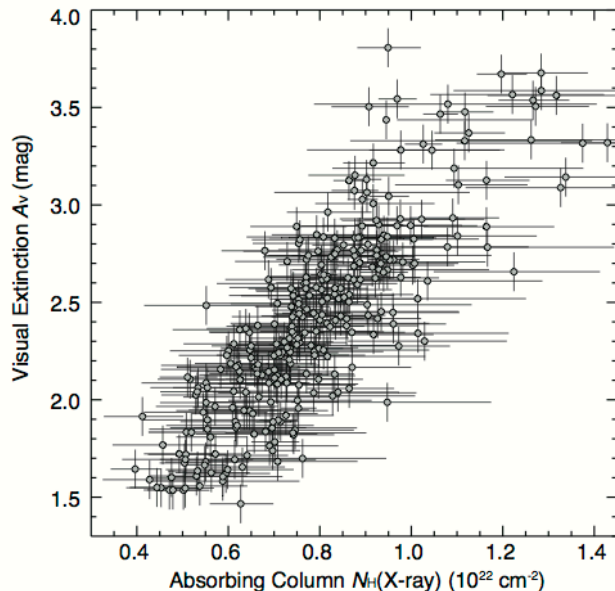
- Maps of the Best-fit parameters
 - (a) absorbing column $N_{\text{H}}(\text{X-ray})$
 - (b) photon index Γ
 - (c) absorption-corrected X-ray flux (3–10 keV)

(contours indicate the smoothed XIS 1–5 keV image)
- Relative error (90% confidence level)
 - $N_{\text{H}}(\text{X-ray}) \dots \sim 14\%$ (max 30%)
 - $\Gamma \dots \sim 6\%$ (max 13%)
 - Flux $\dots \sim 7\%$ (max 23%)

Absorbing column & Visual extinction



Sano+13b in prep.



↑Maps of N_{H} (X-ray) and visual extinction (Dobashi+05)

← Correlation plot

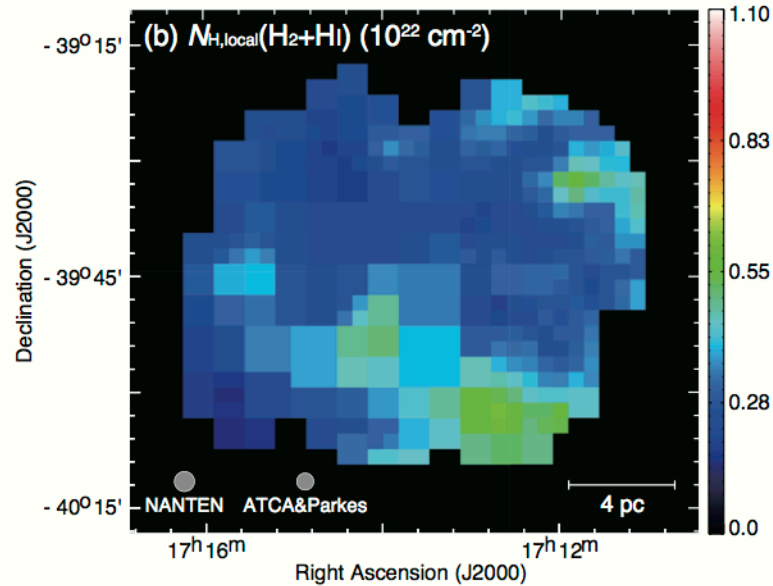
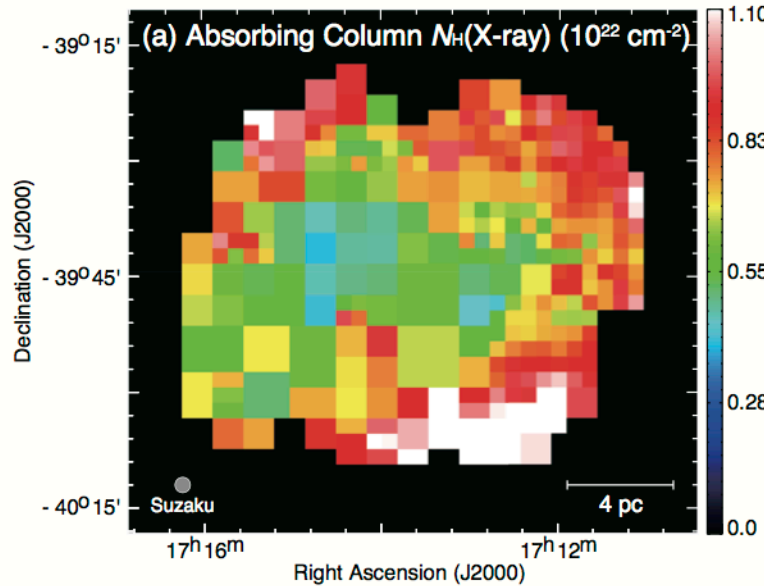
- correlation coefficient: ~0.83
- $N_{\text{H}}(\text{X-rays}) (\text{cm}^{-2}) = 3.0 \times 10^{21} \cdot A_v (\text{mag.})$

cf. $N_{\text{H}} (\text{cm}^{-2}) = 2.5 \times 10^{21} \cdot A_v (\text{mag.})$ (Jenkins & Savage+74)

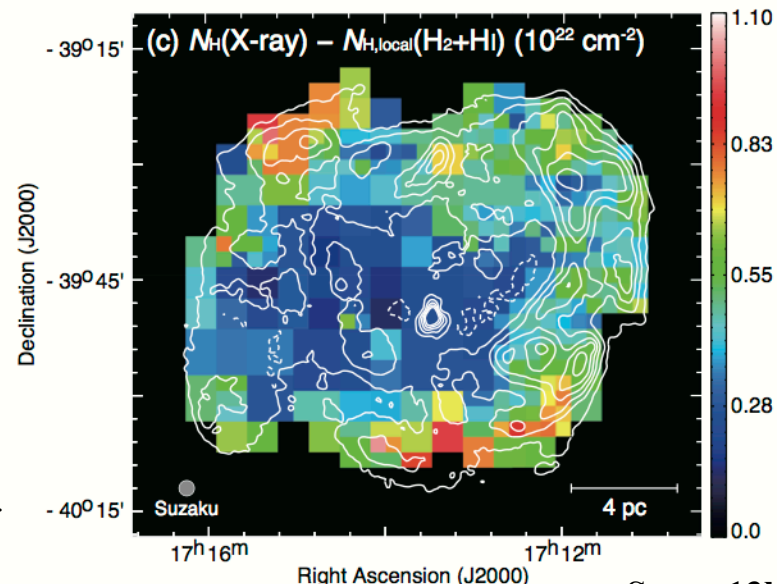
- $N_{\text{H}}(\text{X-rays}) \sim 0.4 - 1.4 \times 10^{22} \text{ cm}^{-2}$ の範囲で変化
→ Cassam-Chenai+04の傾向とconsistent
- $N_{\text{H}}(\text{X-rays})$ と Visual Extinction の非常に良い相関

Absorbing column – Foreground component

12/21

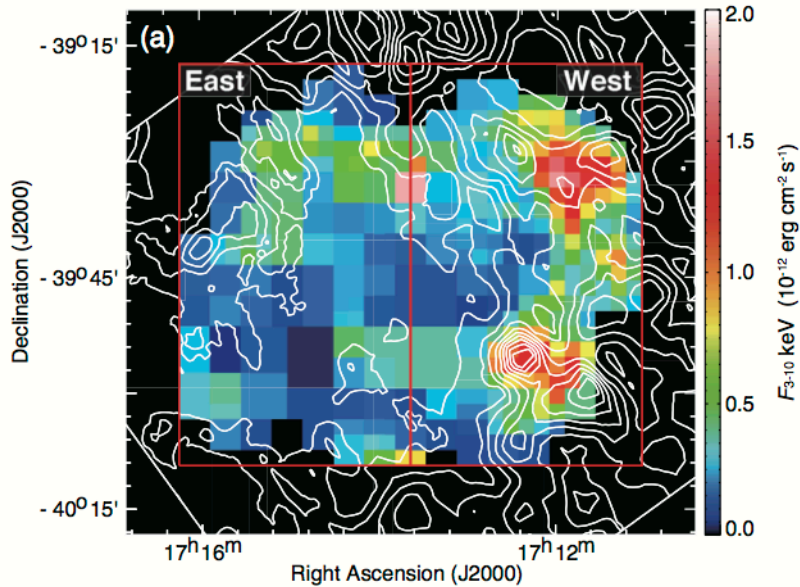


- Foreground component $N_{\text{H},\text{local}}(\text{H}_2+\text{Hi})$ is identified by Moriguchi+05 with NANTEN and *ROSAT* data.
- ISM proton column density estimation
 - $N_{\text{H}}(\text{H}_2+\text{Hi}) = 2 \times N(\text{H}_2) + N_{\text{H}}(\text{Hi})$.
 - $N(\text{H}_2)$ (cm^{-2}) = X_{CO} ($\text{cm}^{-2} (\text{K km s}^{-1})^{-1}$) $\times W(\text{CO})$ (K km s^{-1}).
 - $X_{\text{CO}} = 2 \times 10^{20}$ ($\text{cm}^{-2} (\text{K km s}^{-1})^{-1}$) (Bertsch+93).
- Foreground (local) ISM による吸収量を推定, $N_{\text{H}}(\text{X-ray})$ から差し引く (=SNRとの相互作用分). → X-ray shell に沿った構造が明らかになった.



X-ray Flux & ISM proton column density

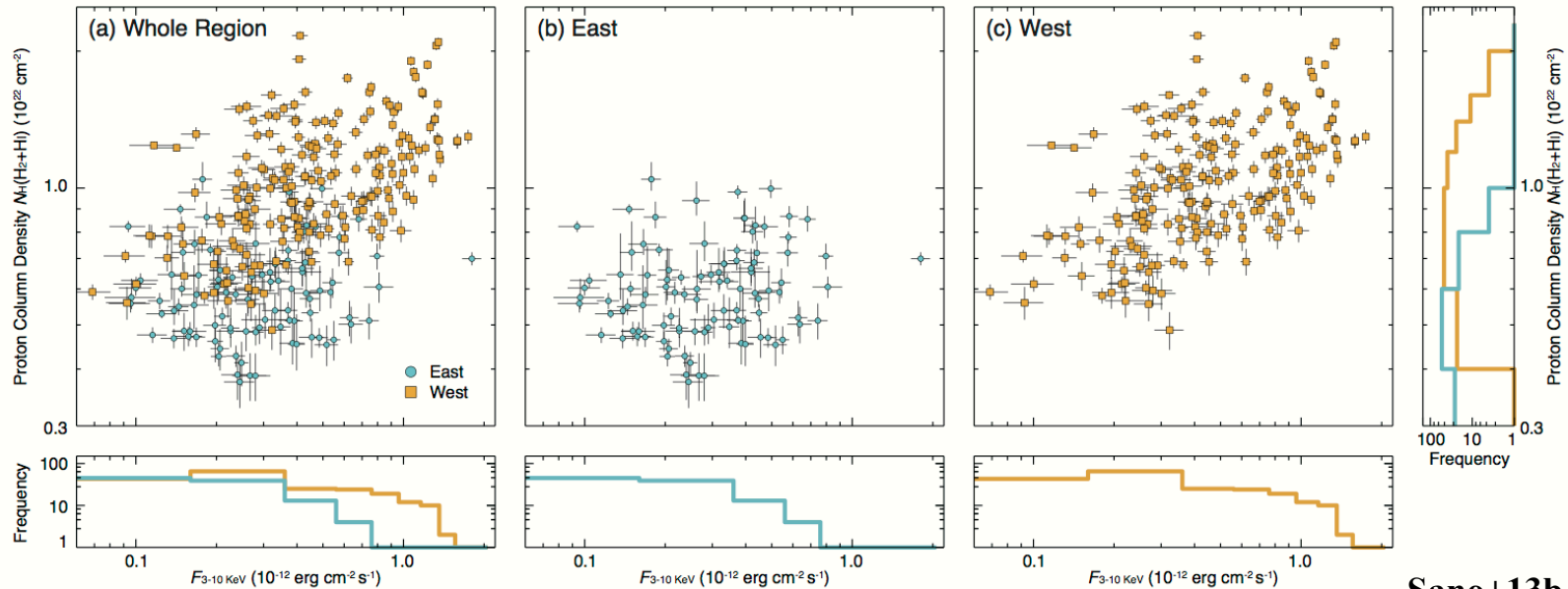
13/21



← Image: absorption-corrected X-ray flux (3–10 keV)
Contours: ISM proton column density $N_{\text{H}}(\text{H}_2+\text{H}_\text{I})$

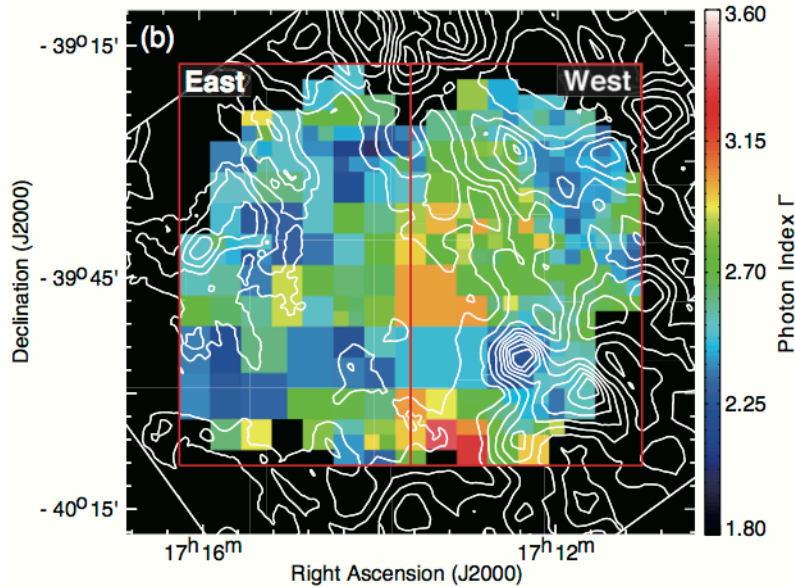
↓ Correlation plot between the Flux and $N_{\text{H}}(\text{H}_2+\text{H}_\text{I})$
(a) whole, (b) East and (c) West region.
Correlation coefficient: ~0.54 (whole region)

- ISMは西側で clumpy, 東側では diffuse に分布.
- ISM の多い領域で X-ray enhance (特に西側)
- 弱いながらも $N_{\text{H}}(\text{H}_2+\text{H}_\text{I})$ と flux は相関



Photon index & ISM proton column density

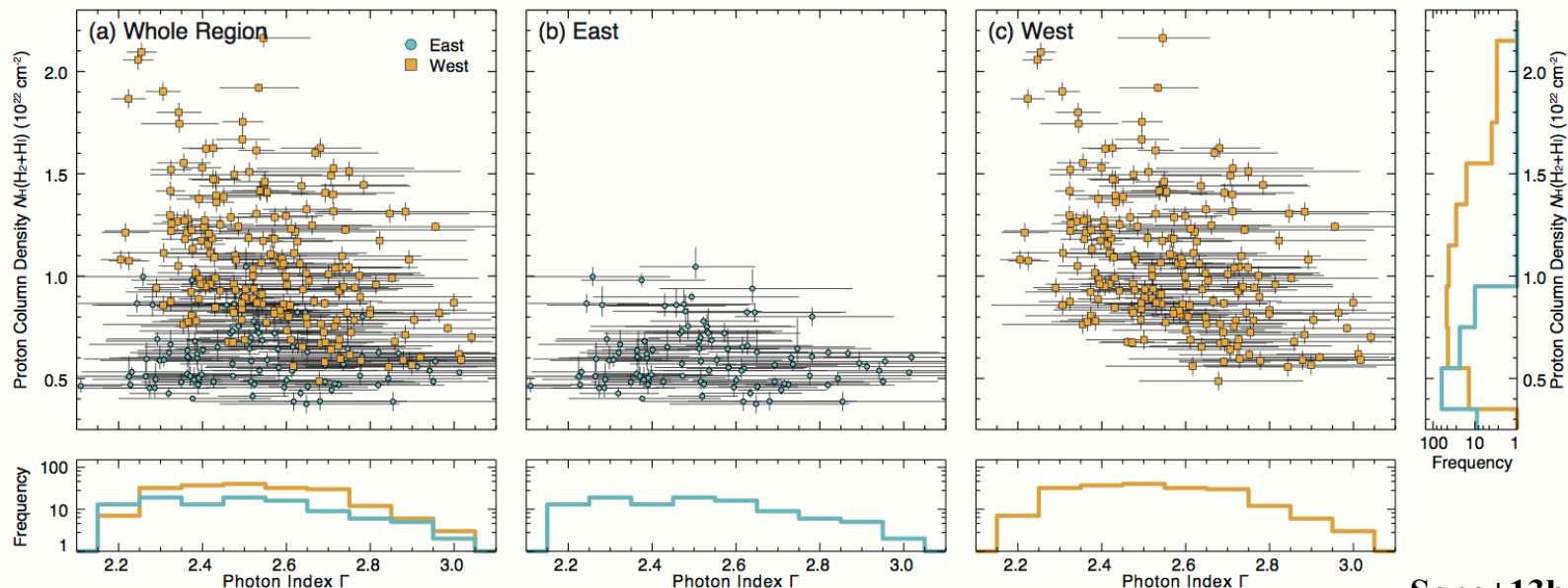
14/21



← Image: Photon index Γ
Contours: ISM proton column density $N_{\text{H}}(\text{H}_2+\text{H}_\text{I})$

↓ Correlation plot between the Γ and $N_{\text{H}}(\text{H}_2+\text{H}_\text{I})$
(a) whole, (b) East and (c) West region.

- SNR 全体に渡って, photon index Γ の小さな領域がいくつか存在している.
- ISM rich な西側は $N_{\text{H}}(\text{H}_2+\text{H}_\text{I})$ と Γ が反相関, 東側では, 両者の顕著な相関は見られない



- We interpret the photon index variation as difference of cut-off energy ε_0 .
 → The cutoff-energy become large (small) when the value of photon index is small (large).
 The cutoff-energy ε_0 is expressed as (Zirakashvili & Aharonian 07),

$$\varepsilon_0 = 0.55 \times (v_s / 3000 \text{ km s}^{-1})^2 \eta^{-1} \text{ keV.}$$

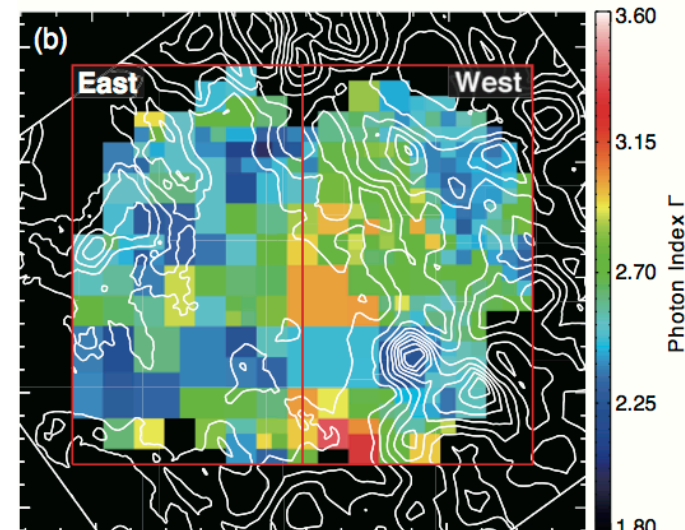
where v_s is shock velocity, η is the degree of magnetic field fluctuations (gyro-factor).

Here, the shock velocity in the dense clump became $v_{s,\text{clump}} = v_{s,\text{ambient}} (n_{\text{ambient}}/n_{\text{clump}})^{0.5}$, where the ambient gas density $n_{\text{ambient}} = 1 \text{ cm}^{-3}$ and clump density $n_{\text{clump}} = 10^2\text{--}10^3 \text{ cm}^{-3}$.

- In the west region: clumpy and rich ISM
 (shock waves will be stalled + strong turbulence)
 ⇒ small shock speed and small η ($\eta \sim 1$; Uchiyama+07)

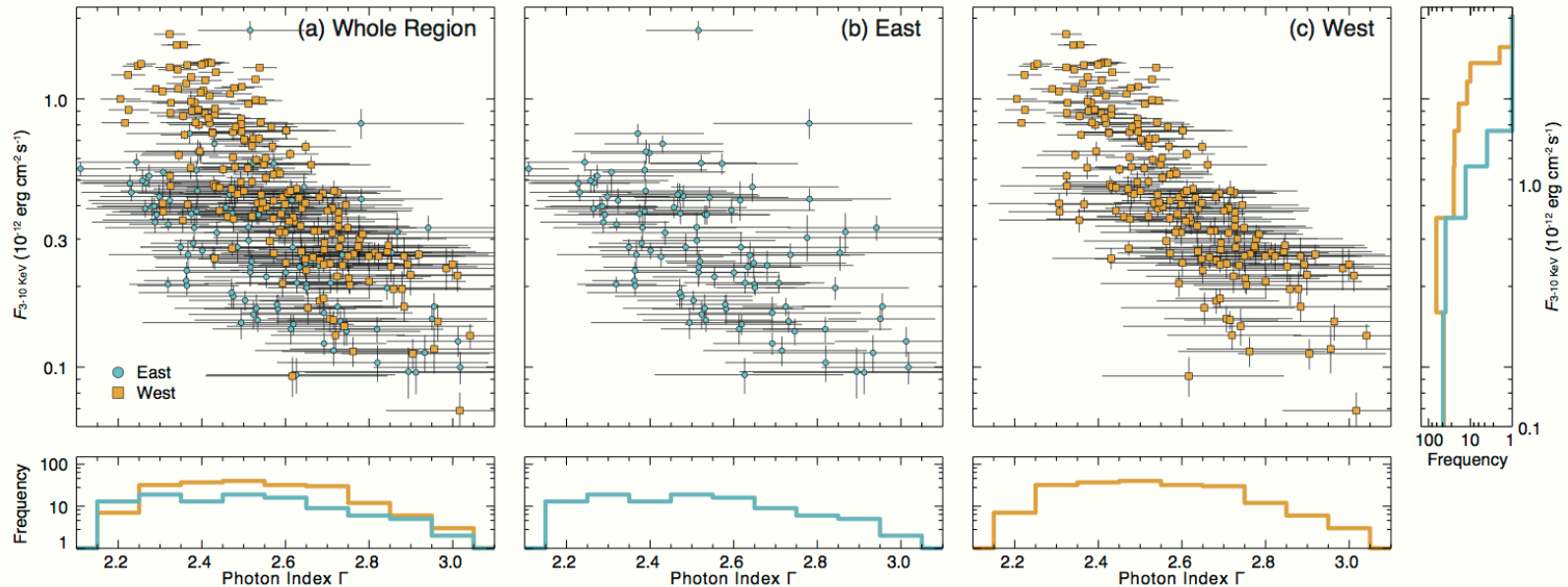
In the east region: diffuse and poor ISM
 (shock waves will be little decelerated)
 ⇒ large shock speed and large η

Therefore, photon index Γ can be small in both regions.
 However, the flux excess cannot describe only this scenario.



Discussion: Efficient cosmic-ray acceleration

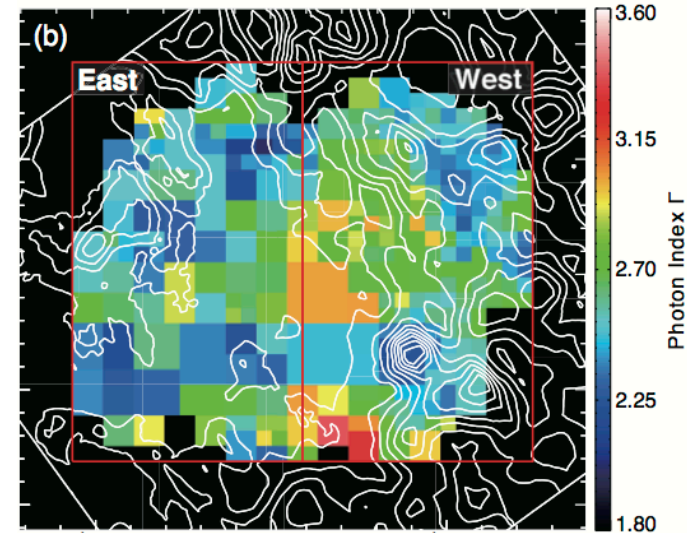
16/21



- In the west region: clumpy and rich ISM
(shock waves will be stalled + strong turbulence)
⇒ small shock speed and small η ($\eta \sim 1$; Uchiyama+07)

- In the east region: diffuse and poor ISM
(shock waves will be little decelerated)
⇒ large shock speed and large η

Therefore, photon index Γ can be small in both regions.
However, the flux excess cannot describe only this scenario.
→ Perhaps the additional particle acceleration mechanism
is working in the ISM rich and clumpy region (e.g., Hoshino+12)



- X-ray spectroscopy for the young TeV γ -ray SNR RXJ1713
 - We reveal the N_{H} (X-ray), Γ and flux maps (+comparing with the ISM)
- Efficient cosmic-ray acceleration
 - We can describe the photon index variation as difference of the cut-off energy.
 - The additional particle acceleration mechanism is working in the ISM rich and clumpy region.
 - The interacting ISM with SNR is crucial play a role to understanding the efficient CR acceleration.
(NANTEN/NANTEN2 CO and *Suzaku* X-ray datasets make a very strong combination!)
- CTA will provide more detail information (high angular resolution images, photon index distribution, etc...) and reveal the relationship between the efficient CR acceleration and the ISM distribution.

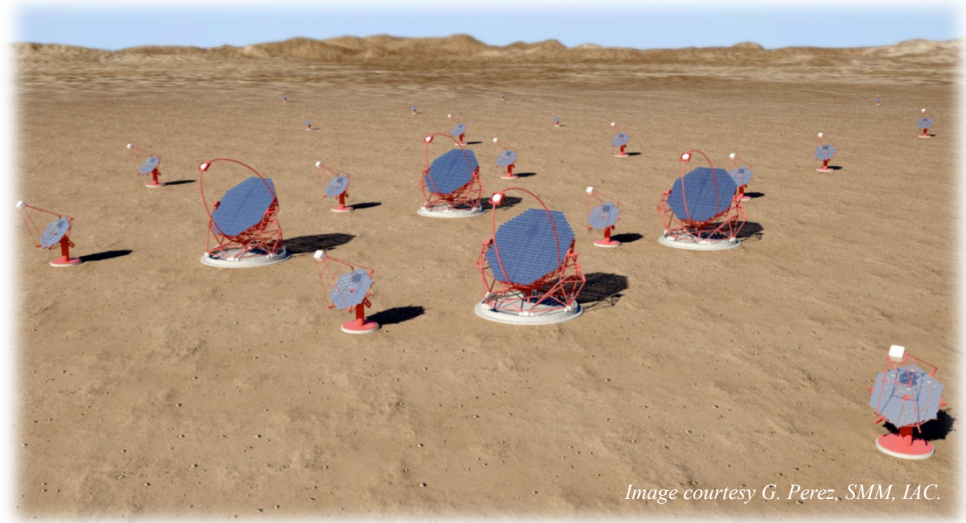
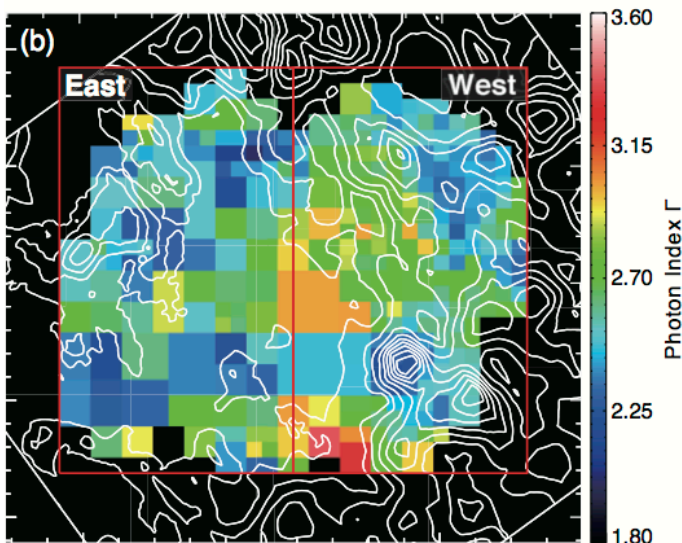
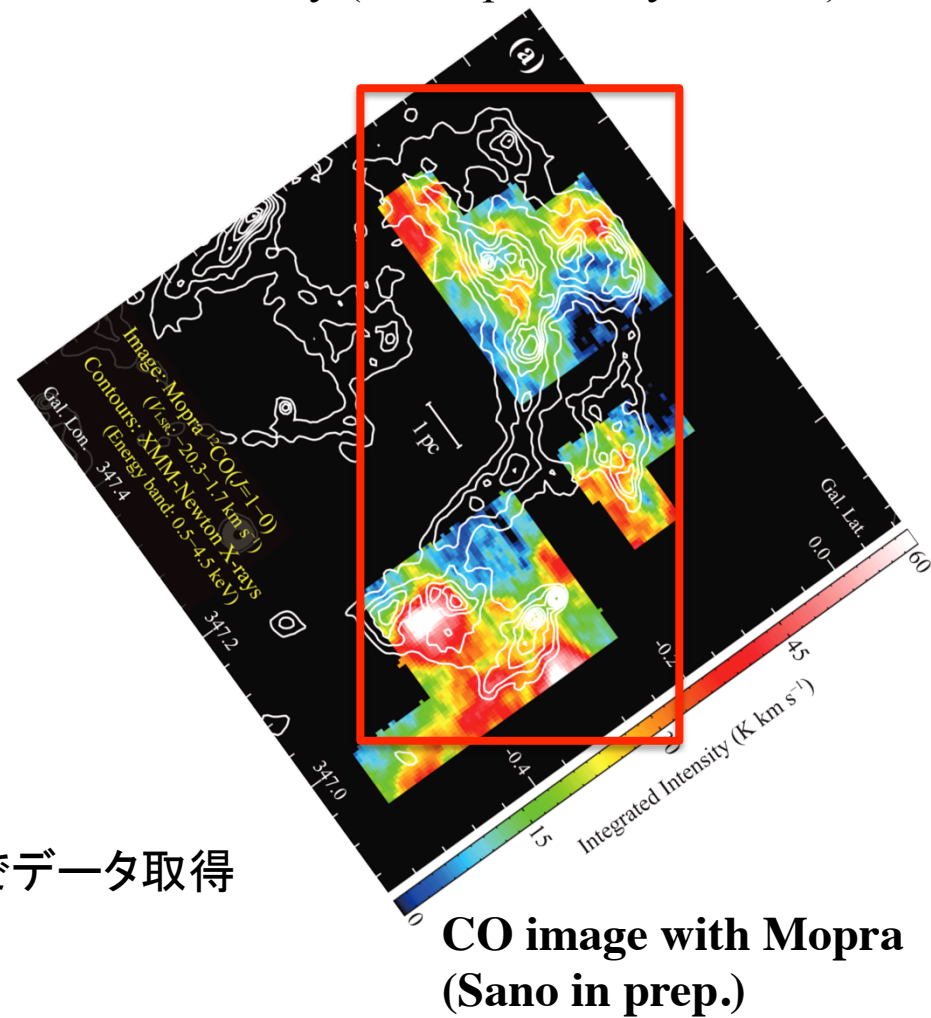
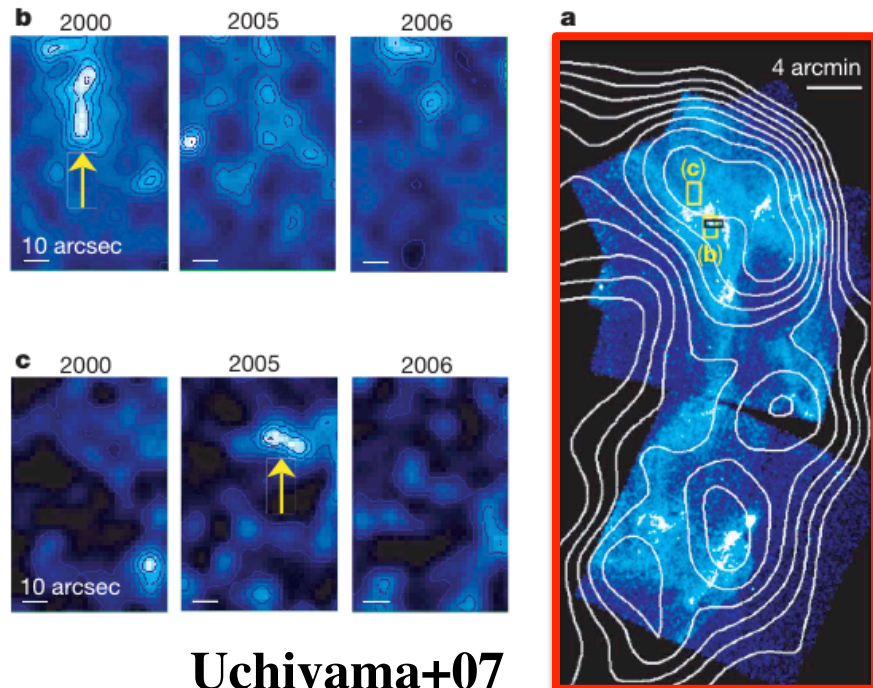


Image courtesy G. Perez, SMM, IAC.

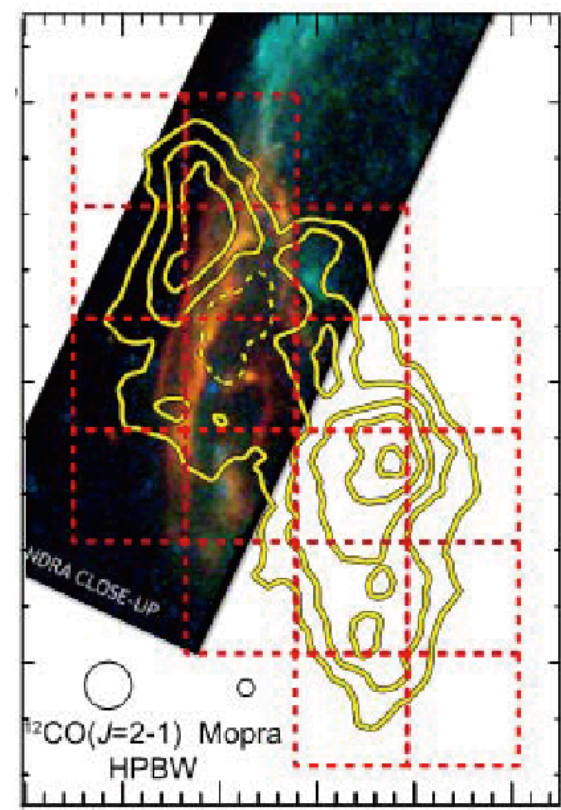
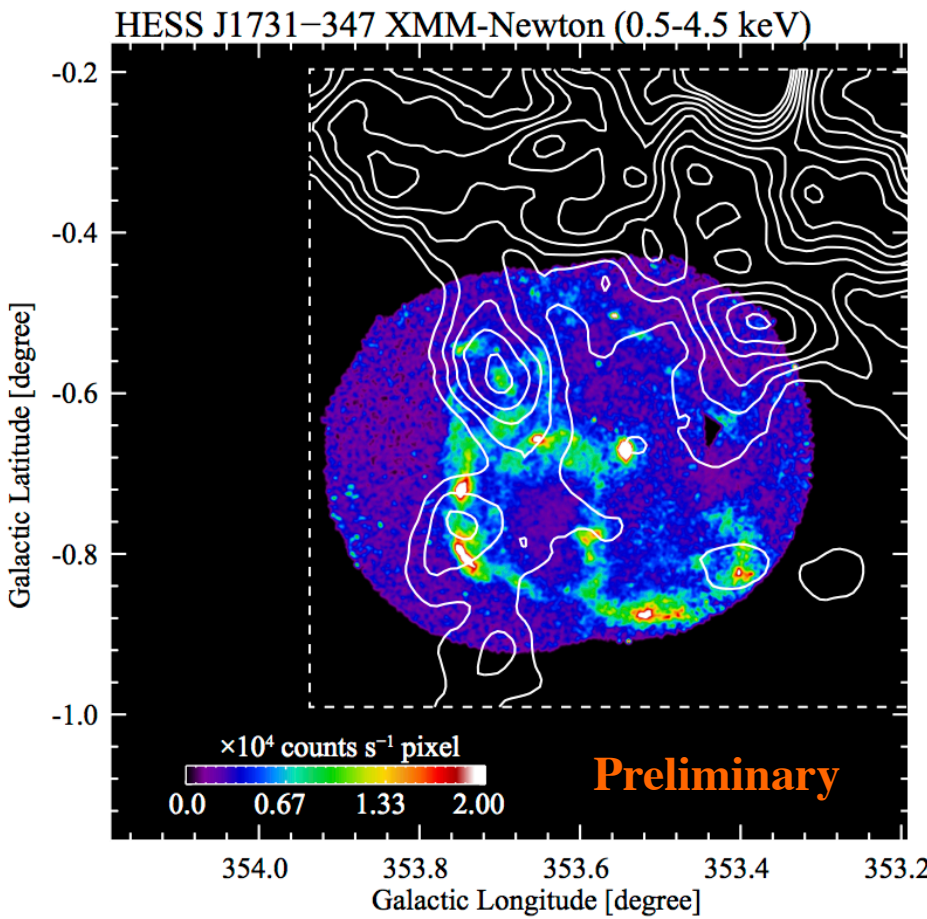
■ RXJ1713 の X-ray filamentary structure と ISM

- MHD 計算の磁場增幅 scale は, ~0.05 pc (Inoue+12).
 - RXJ1713 で確認されているX線の short time variability (~0.05 pc: Uchiyama+07)



■ 他のガンマ線 SNR と ISM の相互作用

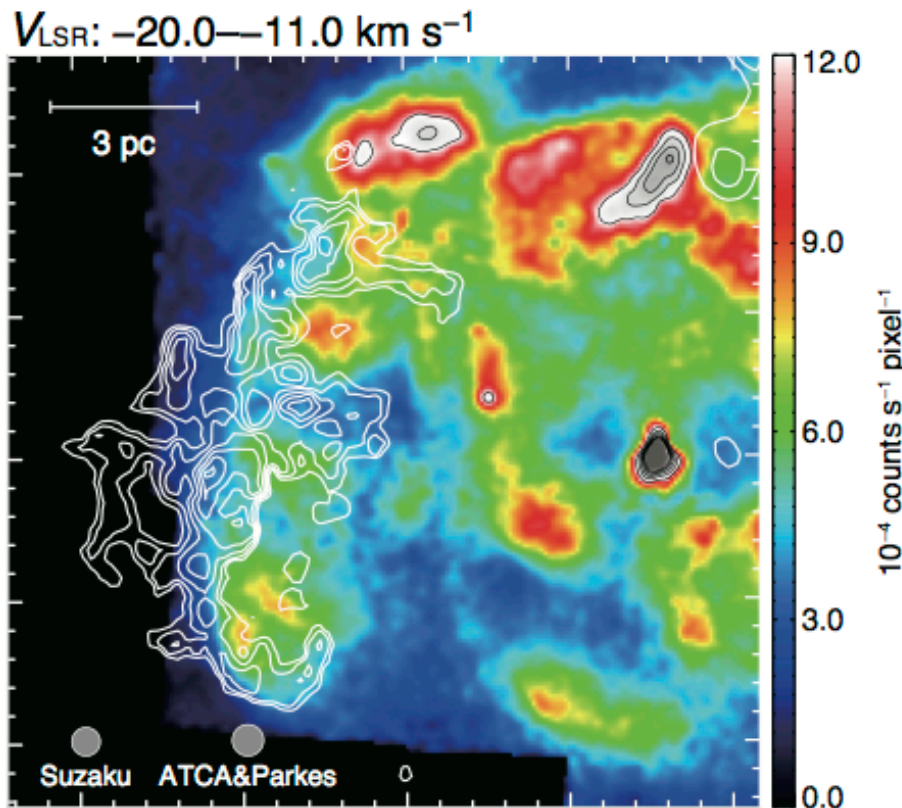
- RXJ1713 の結果の普遍性を探る (HESS J1731, RCW86 etc..)
- Thermal X-rays や Hard X-rays と ISM の関係は? (ASTRO-H SXS, HXI に期待)



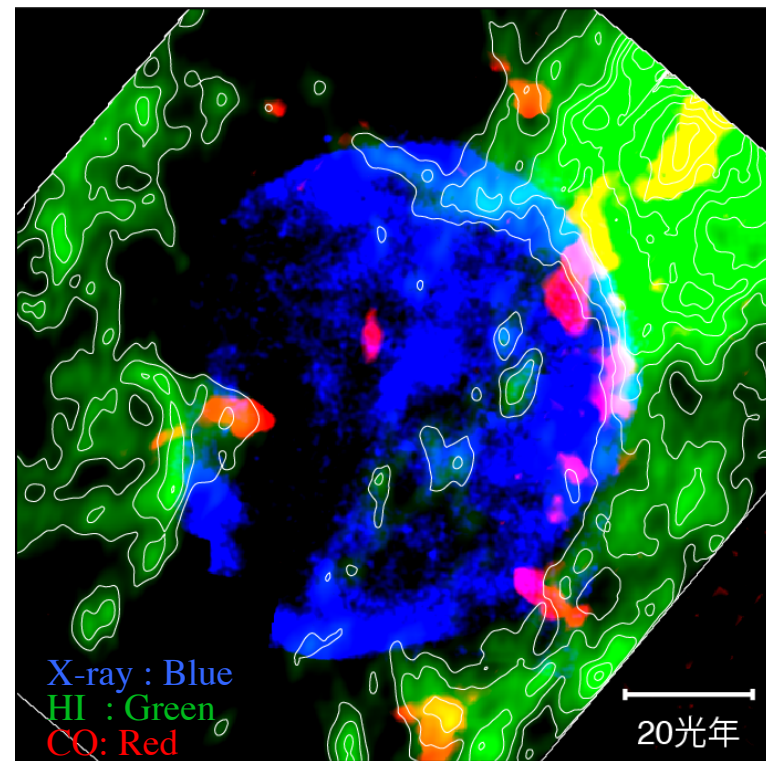
RCW86 X-ray image
+NANTEN2 CO contours

■ Interacting ISM としての HI の重要性

- RXJ1713 SE-rim の cold HI や, Vela Jr. の HI シェルも重要な ISM 構成要素
→ SNR と相互作用する ISM の大半を占めたり, 100 個/cc を超えるものも存在

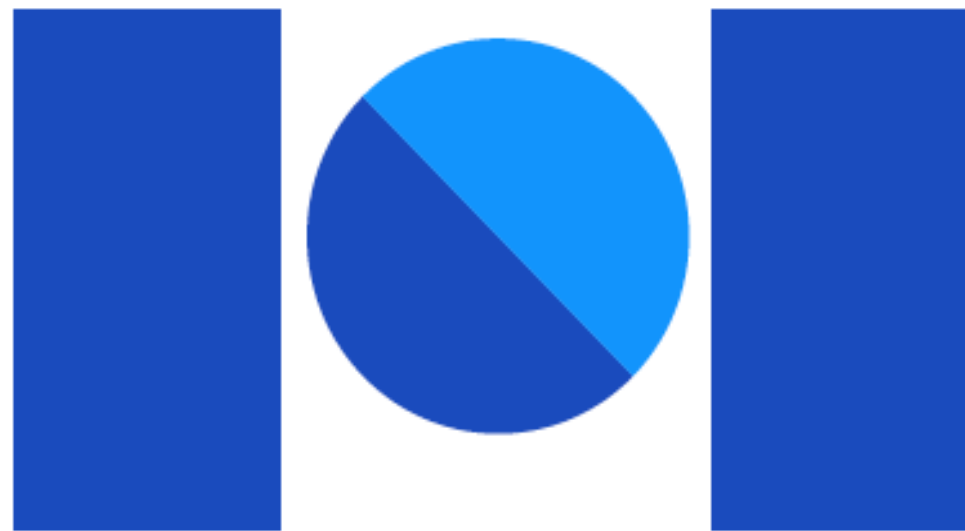


RXJ1713 East (Sano+13b in prep.)



Vela Jr. (Sano+13c in prep.)

多くのSNRについて付随する HI を特定, 物理量を明らかにしていくことが肝要



NANTEN
Submillimeter Observatory